A Hg(I) corrugated sheet assembled by auxiliary dioxole groups and Hg···π interactions†

Francisco Sánchez-Férez, [a] Xavier Solans-Monfort, [a] Teresa Calvet, [b] Mercè Font-Bardia [c] and Josefina Pons *[a]

[a] Departament de Química, Universitat Autònoma de Barcelona ,08193 Barcelona, Spain; E-mail: josefina.pons@uab.es

[b] Departament de Mineralogia, Petrologia i Geologia Aplicada, Universitat de Barcelona, Martí i Franquès s/n, 08028 Barcelona, Spain

[c] Unitat de Difracció de Raig-X, Centres Científics i Tecnològics de la Universitat de Barcelona (CCiTUB), Universitat de Barcelona, Solé i Sabarís, 1-3, 08028 Barcelona, Spain

Abstract

The formation of a new double-stranded staircase Hg(I) supramolecular assembly is reported. It is arranged into 2D corrugated sheets supported by Hg(I)···Odioxole and Hg···π interactions, resulting from the comproportionation reaction between Hg(II) and Hg(0) species in DMF as a solvent.

1. Introduction

Hg as a metal has a particularity of being capable of forming a variety of divalent, trivalent and tetravalent polycations arranged either into linear, dimeric [Hg2]2+, trimeric [Hg3]2+, tetrameric [Hg4]2+ and [Hg]n chains or into [Hg3]4+ triangles or [Hg]n layers.1 All of them present differences in the formation conditions, connectivity, geometry and Hg–Hg bond length. In particular, the formation of the [Hg2]2+ dimeric cation is driven by its slightly positive E° value of +0.115 V which facilitates the comproportionation of Hg2+ and Hg0 into Hg2 2+ as detailed below:2

$$Hg^0 + Hg^{2+} \rightarrow Hg_2^{2+} \qquad E^0 = +0.115\,V$$

This comproportionating ability has been reported to occurin polar solvents, especially in N,N-dimethylformamide (DMF),3 or with strong Lewis bases, inter alia, O- and N-donor ligands.4,5 Although the intrinsic reduction of Hg(II) at high temperature is uncommon, there have been previously reported examples under the mentioned conditions.4 DMF at high temperature can act as a reducing agent,6,7 conducting the formation of Hg0 and triggering comproportionation. The complexation of [Hg2]2+ dimeric cations is usually stabilized by both a lower solubility compared to those of their Hg(II) analogues and the weakening of the donor character of the ligands that minimize the destabilization of the Hg–Hg bond.8 The correlation between Hg–Hg bond length, ranging from 2.495 to 2.557 Å, and the coordinated atoms has been attributed to their electronegativity, being shortened as electronegativity increases. In the presence of an O-donor carboxylate linker, the Hg–Hg distance is enclosed within 2.502–2.557 Å.1 Hg(I) has a strong tendency to form linear arrays due to its soft nature and it usually adopts low coordination numbers of up to four, even though it is capable of accommodating coordination numbers up to seven.9 This preferred linear arrangement facilitates the formation of metal···π interactions which ha ve been proven to be pivotal in defining the arrangement of macromolecules.10 The electrostatic origin of metal···π interactions made them emerge as one of the strongest noncovalent interactions but this strength is highly dependent on the coordinative saturation of the metal, the nature of the π donor aromatic ring and cooperativity with other nonbonding interactions such as hydrogen bonds or π···π stacking.10 In the case of Hg2+, the almost fully populated d orbitals combined with the large s–d orbital energy splitting hinder sd hybridization, albeit evidence of d orbital implication in Hg···π interactions has been reported.11 For this reason, π to Hg donation generally occurs from the molecular orbitals

of the aromatic ring to the unoccupied 6s orbital.12 This favors delocalized π interactions of Hg, with an offset from the centroid ring and placed preferentially over two (πoff(2)) or three carbon atoms (πc(3)), and minimizes those in which Hg is sitting over the center of the ring (πcen(6)). These results were supported by a statistical analysis on metal···π interactions which reinforced the hypothesis that transition metals preferred an offset over the center of the ring in delocalized π interactions.13 Thus far, there are about 28 structures containing the [Hg2]2+ species being coordinated to O atoms.14 From them, six were constructed from carboxylate linkers, inter alia, two alaninates,15 one trifluoroacetate,16 one acetate,17 one gluconate18 and one phthalate,19 all presenting 1D polymeric structures. Above all, only [Hg2(o-phthalate)2]n is arranged through an aromatic carboxylate. Examples of interactions or coordination of dioxole groups to metal centers are scarce and only d10 metal ions have exhibited such an ability. A reported case in the literature with Zn(II)20 and one in our group with Hg(II)21 have been found hitherto. In our case, Hg(II)–Odioxole promoted the formation of a 3D supramolecular assembly. Therefore, the coordination chemistry and structural arrangement of Hg(I) with aromatic carboxylates have not been extensively explored, even less in presence of dioxole groups. In this work, we provide an example of a Hg(I) aromatic carboxylate complex, which is assembled by Hg(I)···O interactions, further expanded into a 3D supramolecular structure by Hg···π and Hg(I)···Odioxole interactions. The formation of the [Hg2]2+ dimeric cation was observed after recrystallization of [Hg(Pip)2IJ4,4′ -bipy)]n (1) in DMF as a solvent at 105 °C for 1 h.22 Under these conditions, the formation of Hg(0) is observed, which combined with the remaining Hg(II) in solution comproportionates to give the [Hg2]2+ species. Subsequent complexation with Pip ligands results in a less soluble compound that gradually nucleates and forms single crystals of [Hg2(Pip)2] (2).

Complex 2 has been characterized by elemental analysis, FTIR-ATR and 1H NMR spectroscopy (ESI† Fig. S1 and S2), and single crystal X-ray diffraction (see details in the ESI†). The deprotonation and subsequent coordination of the Pip linker have been traced from the vanishing of the ν (C ═ O)COOH band and the rise of bands attributable to νas(COO) at 1580 cm−1 and νs(COO) at 1431 cm−1. The coordination modes of the carboxylate can be inferred by calculating the Δ value (Δ = νas(COO) – νs(COO)), which was found to be 149 cm−1 falling in the mid-range between bidentate bridging and bidentate chelate coordination mode, which has been reported for carboxylates with strong interactions.23 Therefore, these results agree with the structural data obtained from the

single crystal X-ray diffraction method. The 1H NMR spectrum in DMSO-d6 displays the aromatic signals of Pip at 7.53, 7.35 and 6.96 ppm and –CH2– at 6.08 ppm (free HPip: 7.55, 7.36, 6.99, 6.11 ppm).

It crystallizes in the monoclinic P21/n space group (ESI† Table S1) and it is composed of linear [Hg2(Pip)2] units that hold two monodentate (μ1-η1) Pip ligands (Fig. 1a), with a coordination number of 2 (Hg1–O1, 2.132(2) Å, and Hg2–O5, 2.126(2) Å, which are below the sum of their covalent radii of 2.21 Å),24 displaying a Hg–Hg bond length of 2.51602(18) Å (Fig. 1a), which falls within the reported range between 2.502 and 2.557 Å.1 Distances below the van der Waals sum of radii (vdWs, from 2.21 to 3.02 Å) have previously been included defining the secondary coordination number,25 but herein have been rather considered as interactions (Hg1···O2, 2.742(2) Å; Hg1···O6, 2.782(2) Å; and Hg1···O5, 3.013(2) Å and Hg2···O6, 2.891(2) Å). The [Hg2(Pip)2] units are joined together in tetrameric [Hg4(Pip)4] assemblies by Pip ligands through Hg1···O2, 2.742(2) Å, and Hg2···O6, 2.891(2) Å, and supported by C–H···O interactions between Pip ligands (Fig. 1b). These [Hg4(Pip)4] clusters are further expanded into a 1D double-stranded staircase assembly along the b axis through Hg1···O5, 3.013(2) Å (Fig. 2a). This arrangement is supported by delocalized Hg1··· πoff(2) and Hg2···πc(3) interactions occurring within the supramolecular chains (Fig. 2b), which display highlighted regions over the aromatic rings in Hirshfeld surface analysis and a 9.6% Hg···C contact surface area contribution in the 2D fingerprint plot (ESI† Fig. S3). These chains are assembled into 2D corrugated sheets through two Hg(I)–Odioxole interactions (Hg1–O7, 3.081(2) Å, and Hg2–O4, 3.132 Å) complemented by double C–H···O interactions between the Pip ligands (Fig. 3, Table S2†). DFT (B3LYP-D2)26–28 calculations have been performed to analyze the interactions between [Hg2(Pip)2] dimers. For that, two sets of calculations were carried out: first, a full periodic calculation of the crystal structure to determine the existing interactions through Bader's quantum theory of atoms in molecules (QTAIM)29–31 and, secondly, finite molecular calculations of all potential close [Hg2(Pip)2] units to quantify the interaction strength between dimers. Both sets of calculations were done with the Crystal17 package,32 and the basis sets were similar to those used for describing related Hg complexes (see the ESI†).33 Fig. 4 shows the four models constructed to determine the interaction strength between dimers, the corresponding interaction energies (with and without Grimme's correction), and the bond critical points (BCPs) involving Hg centres. Table S3† reports the main properties for the BCPs involving Hg.

According to the topological analysis performed with TOPOND, there are BCPs between the two Hg units, Hg and the nearest O atoms either assembling dimers in chains (Fig. 4a), forming tetrameric units (Fig. 4b) and those implying the dioxole fragments (Fig. 4c and d), as well as a BCP located in between Hg and the closest aromatic ring. The presence of these BCPs is indicative of Hg–Hg, Hg–O and Hg···π interactions. The electron density and its Laplacian in the BCPs between Hg and the oxygen atoms or Hg and the aromatic ring indicate that the interaction is mainly of electrostatic and/or van der Waals nature. The computed interaction energies between dimers range from 184.8 to 95.6 kJ mol−1. The strongest interaction is found for dimers assembling into chains by Hg1···O5 and Hg···π interactions, while the weakest interactions take place through the dioxoles. Interestingly, while the Hg···O interaction in tetrameric units is marginally stronger than the Hg···O interaction in the assembly in chains, the Hg···π interaction, only present in the latter case, is of the same order of magnitude and this makes the stabilization by chain formation greater than the formation of in-plane tetramers. The importance of metal···π interactions and their effect on the final arrangement have already been demonstrated10,34 but no results were found regarding the [Hg2]2+ cation. A search in the Cambridge Structural Database (CSD)35 of structures containing the [Hg2]2+ cation and N, O, S and P-donor atoms resulted in 129 hits. Disordered structures were eliminated in order to include only precise crystal structure determinations. The data were sifted through those with aromatic rings and were reduced to a total of 50 entries with potential Hg···π interactions. One essential requirement is that the metal acceptor has a coordinatively unsaturated environment that allows the bulky aromatic ring to get closer. The vast majority presents crowded structures with coordination numbers of 2 with secondary interactions of up to 7 [2 + 5]9 with solvent molecules either below or over their vdWs, which hinders Hg(I)···π interactions. Besides, in some examples, the geometric preferences of the ligands hamper the proper orientation of the aromatic rings towards the [Hg2]2+ cation.5 Of them, only 9 hits presented delocalized π interactions with [Hg2]2+, considering either a Hg(I) to benzene plane distance (dHgP) below the vdWs of the Hg and C atoms (3.45 Å)11 or a Hg(I) to centroid distance below 4.0 Å.13 For all the structures, each Hg···π interaction has been split into the coordination number of the Hg(I) atom, the distances between Hg and i) the nearest C atoms (dHgC); ii) the ring centroid (dHgCg); iii) the plane containing the aromatic ring (dHgP); the offset, which is defined as $\sqrt{\left(d_{HgCg}^2 - d_{HgP}^2\right)}$ (ref. 13) and the conformation,12 resulting in 14 Hg(I)···π interactions. Each interaction with the mentioned parameters is summarized in Table 1.

The general trend is that an offset of the Hg(I) center over sitting in the ring centroid axis is preferred, with πc(η3) being slightly favored over πoff(2). Only [Hg2(o-phthalate)2]n (A) presents a small offset of 0.5274 Å and exhibits a πcen(6) conformation. Among them, E, G and I present Hg(I)···π···π cooperativity, which is reported to be a prevailing motif by enhancing the strength of the π···π interaction.10 The πoff(2) and πc(3) conformations are present in the remaining structures (B, C, D, F, H) with offset values from 0.9305 to 2.024 Å and between 1.243 and 1.516 Å, respectively. It can be inferred that the πc(3) conformation (B, C, F, G, H and I) limits the offset range by anchoring the Hg(I) ion and preventing it from being placed out of the aromatic ring. The smallest offsets have been found in complexes 2 and A, both bearing structures that predispose Hg(I) atoms to sit closer to the centroid of the aromatic ring. Besides, the interaction of the dioxole O atoms to Hg1 in 2 reduces Hg···π, resulting in πoff(2) while the coordinatively unsaturated Hg1 can accommodate the πc(3) interaction.

2. Conclusions

The use of DMF as a solvent and the decomposition of precursor 1 to give Hg(0) have driven the formation of the [Hg2]2+ cation, which after coordination with the Pip linker has been stabilized through precipitation due to the low solubility of complex 2. Hg···O and Hg···π interactions cooperate in the formation of double-stranded staircase chains, which are connected into 2D sheets by an uncommon Hg(I)···Odioxole interaction. DFT calculations between dimers showed that the significant stabilization energy of Hg···π associations and their topological analysis ensured the formation of the [Hg2]2+ cation as well as Hg···O interactions either from carboxylates or dioxole groups. Besides, literature results of Hg(I)···π interactions have been compiled and analyzed, revealing that the πc(3) conformation is slightly preferred over πoff(2) for the [Hg2]2+ cation.

Author Contributions

Conceptualization, J. P.; data curation, F. S.-F., X. S.-M and M. F.-B.; formal analysis, F. S.-F. and M. F.-B.; funding acquisition, X. S.-M. and J. P.; investigation, F. S.- F.; methodology, F. S.-F. and X. S.-M.; project administration, X. S.-M. and J. P.; resources, X. S.-M., T.C. and J. P.; software, F. S.-F. and X. S.-M.; supervision, J. P.; validation, X. S.-M., T. C. and J. P.; visualization, F. S.-F.; writing – original draft, F. S.-F.; writing – review and editing, X. S.-M., T. C. and J. P.

Conflicts of Interest

There are no conflicts to declare.

Acknowledgements

J. P. acknowledges financial support from the CB615921 project, the CB616406 project from "Fundació La Caixa" and the 2017SGR1687 project from the Generalitat de Catalunya. X. S.-M. acknowledges financial support from MICINN (PID2020-112715GB-I00) and the Generalitat de Catalunya (2017SGR1323). F. S.-F. acknowledges the PIF pre-doctoral fellowship from the Universitat Autònoma de Barcelona.

Notes and references

1 L. M. Volkova and S. A. Magarill, J. Struct. Chem., 1999, 40, 262–269.

2 R. A. Jackson, The chemistry of mercury, The Macmillan Press Ltd, London and Basingstoke, 1st edn, 1978.

3 M. Kadarkaraisamy and A. G. Sykes, Polyhedron, 2007, 26, 1323–1330.

4 N. J. Williams, R. D. Hancock, J. H. Riebenspies, M. Fernandes and A. S. De Sousa, Inorg. Chem., 2009, 48, 11724–11733.

5 D. C. Bebout, J. F. Bush, E. M. Shumann, J. A. Viehweg, M. E. Kastner, D. A. Parrish and S. M. Baldwin, J. Chem. Crystallogr., 2003, 33, 457–463.

6 J. Muzart, Tetrahedron, 2009, 65, 8313–8323.

7 M. M. Heravi, M. Ghavidel and L. Mohammadkhani, RSC Adv., 2018, 8, 27832–27862.

8 K. Brodersen, Comments Inorg. Chem., 1981, 1, 207–225.

9 K. Brodersen and R. Dolling, Chem. Ber., 1978, 111, 3354–3359.

10 A. S. Mahadevi and G. N. Sastry, Chem. Rev., 2013, 113, 2100–2138.

11 A. Lannes, A. Manceau, M. Rovezzi, P. Glatzel, Y. Joly and I. Gautier-Luneau, Dalton Trans., 2016, 45, 14035–14038.

12 H. B. Yi, H. M. Lee and K. S. Kim, J. Chem. Theory Comput., 2009, 5, 1709–1717.

13 A. Banerjee, A. Saha and B. K. Saha, Cryst. Growth Des., 2019, 19, 7264–7270.

14 C. R. Groom, I. J. Bruno, M. P. Lightfoot and S. C. Ward, Acta Crystallogr., Sect. B: Struct. Sci., Cryst. Eng. Mater., 2016, 72, 171–179.

15 C. D. L. Saunders, N. Burford, U. Werner-Zwanziger and R. Mcdonald, Inorg. Chem., 2008, 47, 3693–3699.

16 M. Sikirica and D. Grdenić, Acta Crystallogr., Sect. B: Struct. Crystallogr. Cryst. Chem., 1974, 30, 144–146.

17 T. J. Prior, Acta Crystallogr., Sect. E: Struct. Rep. Online, 2005, 61, m1523–1524.

18 I. G. Konkina, S. P. Ivanov and Y. I. Murinov, Russ. J. Inorg. Chem., 2019, 64, 201–206.

19 B. Lindh, Acta Chem. Scand., 1967, 21, 2743–2752.

20 P. V. Dau, L. R. Polanco and S. M. Cohen, Dalton Trans., 2013, 42, 4013–4018.

21 D. Ejarque, F. Sánchez-Férez, J. A. Ayllón, T. Calvet, M. Font-Bardia and J. Pons, Cryst. Growth Des., 2020, 20, 383–400.

22 F. Sánchez-Férez, X. Solans-Monfort, T. Calvet, M. Font-Bardia and J. Pons, Inorg. Chem., 2022, 61, 4965–4979.

23 G. B. Deacon and R. J. Phillips, Coord. Chem. Rev., 1980, 33, 227–250.

24 J. G. Wright, M. J. Natan, F. M. Macdonnell, D. M. Ralston and T. V. O. Hallorant, in Progress in Inorganic Chemistry, ed. S. J. Lippard, John Wiley & Sons, Hoboken, New Jersey, USA, 2007, pp. 323–412.

25 D. Grdenić, Q. Rev., Chem. Soc., 1965, 19, 303–328.

26 A. D. Becke, Phys. Rev. A: At., Mol., Opt. Phys., 1988, 38, 3098–3100.

27 C. Lee, W. Yang and R. G. Parr, Phys. Rev. B: Condens. Matter Mater. Phys., 1988, 37, 785–789.

28 S. Grimme, J. Comput. Chem., 2012, 27, 1787–1799.

29 H. J. Bohórquez, R. J. Boyd and C. F. Matta, J. Phys. Chem. A, 2011, 115, 12991–12997.

30 R. F. W. Bader, Acc. Chem. Res., 1985, 18, 9–15.

31 R. F. W. Bader, Chem. Rev., 1991, 91, 893–928.

32 R. Dovesi, A. Erba, R. Orlando, C. M. Zicovich-Wilson, B. Civalleri, L. Maschio, M. Rérat, S. Casassa, J. Baima, S. Salustro and B. Kirtman, Wiley Interdiscip. Rev.: Comput. Mol. Sci., 2018, 8, 1–36.

33 A. Giordana, E. Priola, S. Pantaleone, L. Andreo, L. Mortati, P. Benzi, L. Operti and E. Diana, Dalton Trans., 2022, 51, 5296–5308.

34 H. Lee, H. S. Lee, J. H. Reibenspies and R. D. Hancock, Inorg. Chem., 2012, 51, 10904–10915.

35 C. R. Groom, I. J. Bruno, M. P. Lightfoot and S. C. Ward, Acta Crystallogr., Sect. B: Struct. Sci., Cryst. Eng. Mater., 2016, 72, 171–179.

36 N. B. Padalwar and K. Vidyasagar, J. Solid State Chem., 2016, 243, 83–94.

37 J. Hicks, E. J. Underhill, C. E. Kefalidis, L. Maron and C. Jones, Angew. Chem., Int. Ed., 2015, 54, 10000–10004.

38 S. P. Argent, H. Adams, T. Riis-Johannessen, J. C. Jeffery, L. P. Harding, W. Clegg, R. W. Harrington and M. D. Ward, Dalton Trans., 2006, 4996–5013.

39 M. Juckel, D. Dange, C. de Bruin-Dickason and C. Jones, Z. Anorg. Allg. Chem., 2020, 646, 603–608.

40 F. Xu, Y. X. Peng, B. Hu, T. Tao and W. Huang, CrystEngComm, 2012, 14, 8023–8032.

Table 1. CSD results of the selected structures exhibiting Hg(I)···π interactions

Complex	CN[a]	d_{HgC} (Å)	d_{HgCg} (Å)	d_{HgP} (Å)	Offset[b] (Å)	Conformation	Ref.
$[Hg_2(Pip)_2]$ (**2**)	2	3.405(3); 3.488(3);	3.720[c]	3.342	1.634	$\pi_{off}(2) + \pi_c(3)$	This work
		3.358(3); 3.460(3); 3.647(3)	3.446[d]	3.318	0.9305		
$[Hg_2(o\text{-phthalate})_2]_n$ (**A**)	2	3.335; 3.419; 3.469; 3.646; 3.687; 3.737	3.256[e]	3.213	0.5274	$\pi_{cen}(6) + \pi_{off}(2)$	19
		3.341; 3.459	3.801[e]	3.217	2.024		
$(Hg_2)Hg_3(O_3P(C_6H_4)PO_3)_2{\cdot}2H_2O$ (**B**)	2	3.12(2); 3.41(2); 3.45(2)	3.424[f]	3.137	1.372	$\pi_c(3)$	36
$Hg_2(N(Ar)(SiMe_3))_2$ (**C**)	2	3.155(3); 3.361(3); 3.458(4)	3.380[g]	3.143	1.243	$\pi_c(3)$	37
$Hg_2(N(Ar)(SiPr^i_3))_2$ (**D**)	2	3.413(6); 3.458(5)	3.620[h]	3.362	1.342	$\pi_{off}(2)$	
$[Hg_2(L^{oPh})]{\cdot}(ClO_4)_2{\cdot}(CH_3NO_2)$ (**E**)	3	3.37(3); 3.63(3)	3.817[i]	3.301	1.917	$\pi_{off}(2)$	38
$[Hg_2(L^{mPh})(DMF)_2]{\cdot}(ClO_4)_2$ (**F**)	3	3.478(6); 3.672(6); 3.788(8)	3.732[j]	3.466	1.384	$\pi_c(3) + \pi_{off}(2)$	
		3.524(7); 3.575(8);	3.721[j]	3.476	1.328		
		3.395(8); 3.540(7)	3.836[k]	3.300	1.956		
$[Hg_2(L^{pPh})]{\cdot}(ClO_4)_2$ (**G**)	3	3.28(1); 3.41(1); 3.62(1);	3.485[l]	3.255	1.245	$\pi_c(3) + \pi_{off}(2)$	
		3.51(1); 3.66(1)	3.719[l]	3.497	1.266		
		3.30(1); 3.58(1); 3.61(1)	3.628[m]	3.294	1.521		
$[Hg_2((MesNCMe)_2CH)_2]{\cdot}$hexane (**H**)	2	3.090(4); 3.320(4); 3.510(4);	3.430[n]	3.077	1.516	$\pi_c(3)$	39
		3.081(4); 3.248(4); 3.452(4);	3.322[o]	3.060	1.293		
$[Hg_2(TIP)_2](ClO_4)_2$ (**I**)	3	3.338(6); 3.570(7); 3.590(6);	3.519[p]	3.331	1.135	$\pi_c(3)$	40
		3.428(2); 3.508(6)	3.620[q]	3.341	1.394		

[a] CN = coordination number. [b] Offset = $\sqrt{(d_{MC}{}^2 - d_{MP}{}^2)}$; d_{HgC} = Hg···C atom distance; d_{HgCg} = Hg···centroid distance, d_{HgP} = Hg···plane distance defined by the aromatic ring. [c] centroid: C(2)–C(3)–C(4)–C(5)–C(7)–C(8). [d] centroid: C(10)–C(11)–C(12)–C(14)–C(15)–C(16). [e] centroid: C(2B)–C(3B)–C(4B)–C(5B)–C(6B)–C(7B). [f] centroid: C(1A)–C(2A)–C(3A)–C(4A)–C(5A)–C(6A). [g] centroid: C(10B)–C(15B)–C(16B)–C(17B)–C(34B)–C(37B). [h] centroid: C(10)–C(24)–C(33)–C(40)–C(41)–C(42). [i] centroid: C(1)–C(2)–C(3)–C(4)–C(5)–N(1). [j] centroid: C(10)–C(11)–C(12)–C(13)–C(14)–C(15). [k] centroid: C(1)–C(2)–C(3)–C(4)–C(5)–N(1). [l] centroid: C(10)–C(11)–C(12)–C(13)–C(14)–C(15). [m] centroid: C(44)–C(45)–C(46)–C(47)–C(48)–N(12). [n] centroid: C(15)–C(16)–C(17)–C(18)–C(19)–C(20). [o] centroid: C(44)–C(45)–C(46)–C(47)–C(48)–C(49). [p] centroid: N(3A)–C(4A)–C(5A)–C(6A)–C(13A). [q] centroid: S(1A)–C(14A)–C(15A)–C(16A)–C(17A). ($O_3P(C_6H_4)PO_3)_2$ = 1,4-phenylenebisphosphonic acid; N(Ar)($SiMe_3$) = *N*-(2,6-bis(diphenylmethyl)-4-isopropylphenyl)-1,1,1-trimethylsilanaminato; N(Ar)($SiPr^i_3$) = *N*-(2,6-bis(diphenylmethyl)-4-methylphenyl)-1,1,1-triisopropylsilanaminato; L^{oPh} = 1,2-bis(3-(2-pyridyl)pyrazol-1-ylmethyl)benzene-*N*,*N*′,*N*″,*N*‴; L^{mPh} = 1,3-bis(3-(2-pyridyl)pyrazol-1-ylmethyl)benzene-*N*,*N*′,*N*″,*N*‴; L^{pPh} = 1,4-bis(3-(2-pyridyl)pyrazol-1-ylmethyl)benzene-*N*,*N*′,*N*″,*N*‴; ((MesNCMe)$_2$CH) = 1,3-bis(2,6-diisopropylphenyl)-*N*-(trimethylsilyl)-1,3-dihydro-2*H*-1,3,2-diazaborol-2-amino; TIP = 2-(2-thienyl)-1*H*-imidazo[4,5-*f*][1,10]phenanthroline-N^7,N^8.

Figures Captions

Figure 1. Crystal structure representation of 2. a) Dinuclear [Hg2Pip2] units displaying μ1-η1 coordination modes. b) Tetranuclear [Hg2Pip4] units supported by Hg···O and C–H···O interactions (represented as dashed lines). Color codes: suva grey (Hg), red(O), grey (C) and white (H).

Figure. 2 Views of the a) 1D double-stranded staircase assembly, and b) Hg1··· πoff(2) and Hg2···πc(3) interactions (dashed blue lines). Hg···O interactions are represented as dashed lines.

Figure 3. Views of the assembly of 2D corrugated sheets supported by a) Hg···Odioxole and C–H···O interactions or b) Hg···π and Hg···Odioxole interactions.

Figure 4. Models constructed to analyze the interaction and associated interaction energies (without including dispersion forces in parentheses) of a) dimers interacting via Hg···O and Hg···π; b) dimers forming a tetrameric unit; c) and d) dimers assembled by Hg···Odioxole. The yellow spots correspond to the BCPs involving Hg(I) cations. Values are given in kJ mol−1.

Figure 1

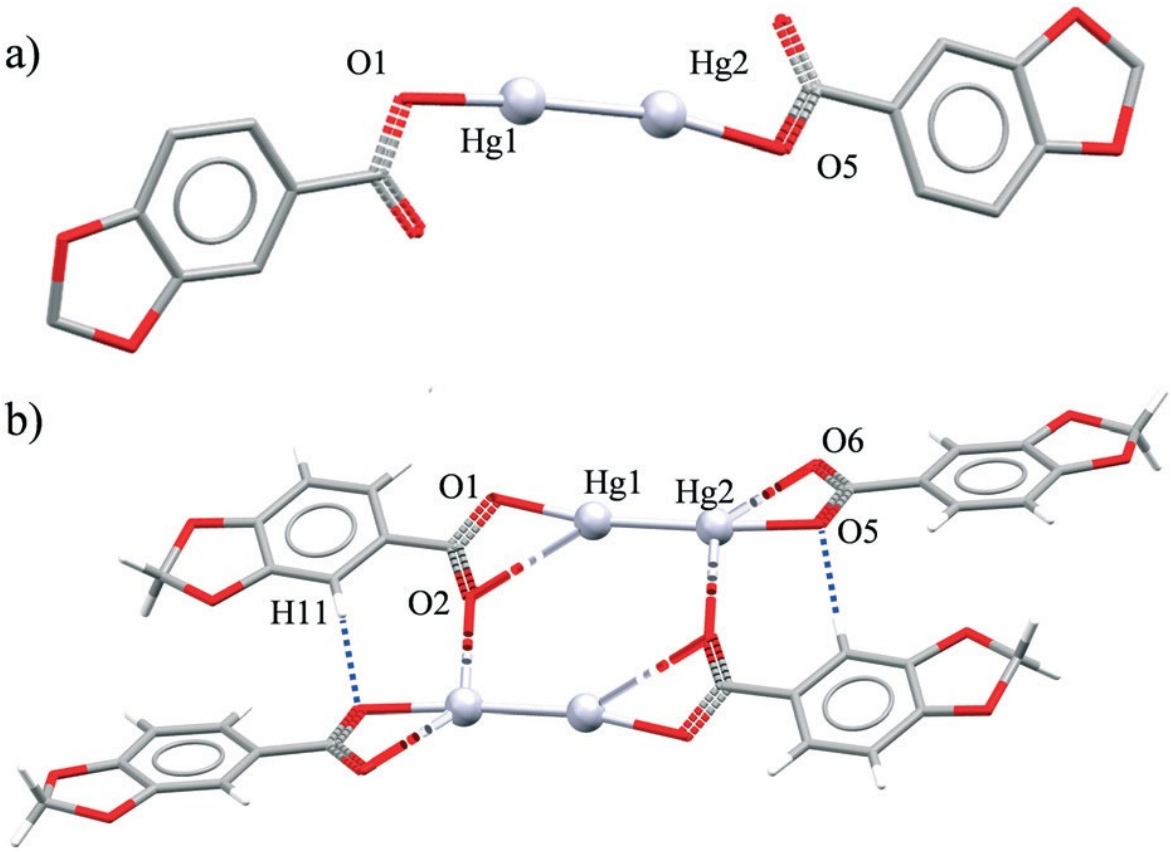

Figure 2

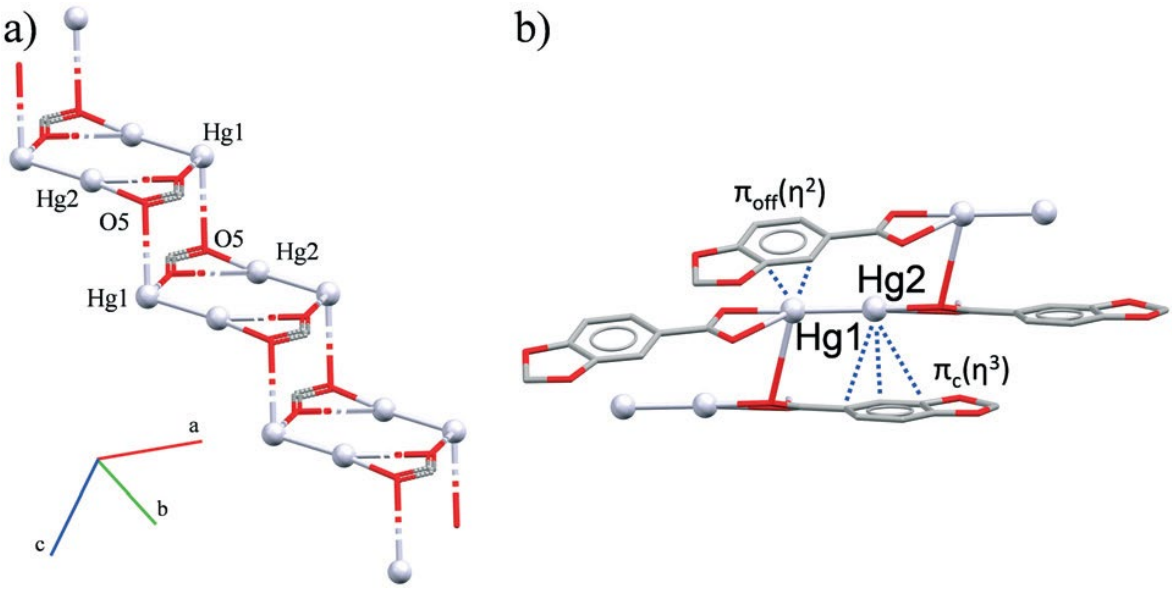

Figure 3

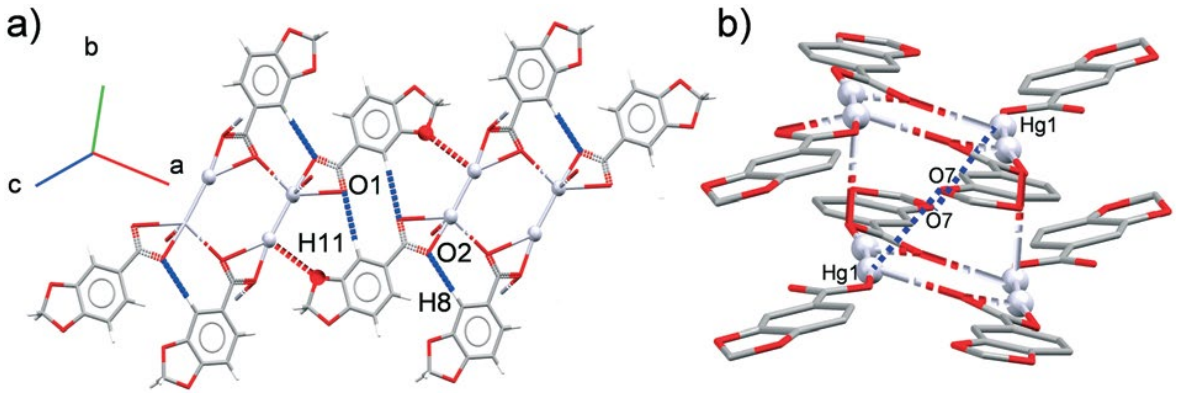

Figure 4

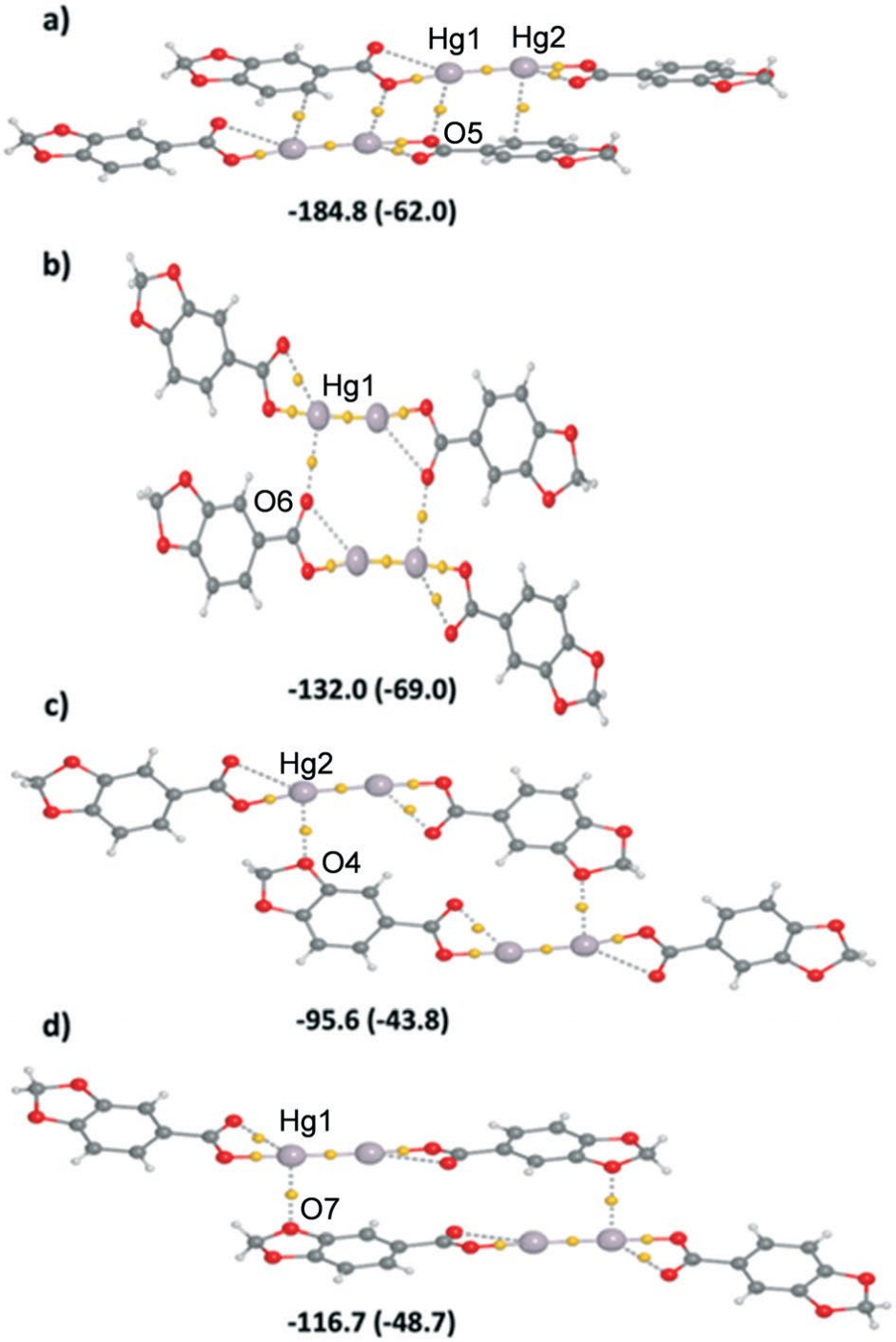
a)
Hg1
Hg2
O5
-184.8 (-62.0)
b)
Hg1
O6
-132.0 (-69.0)
c)
Hg2
O4
-95.6 (-43.8)
d)
Hg1
O7
-116.7 (-48.7)